Starch Fractions as Examples for Nonrandomly Branched Macromolecules. 4. Angular Dependence in Dynamic Light Scattering

Gabriela Galinsky and Walther Burchard*

Institute of Macromolecular Chemistry, University of Freiburg, Sonnenstrasse 5, D-79104 Freiburg, Germany

Received December 3, 1996; Revised Manuscript Received August 15, 1997[⊗]

ABSTRACT: The angular dependence of dynamic light scattering from five degraded potato starch samples was studied. The study allowed the determination of internal modes of motion in branched structures that resemble hyperbranched polymers. The properties of the investigated starches are dominated by the large size of the amylopectin. Measurements were made at infinite dilution ($c = 0$) and at concentrations $c > c^*$ where c^* is the overlap concentration. The time correlation function (TCF) at low concentration was analyzed by its first cumulant at low values of qR_g and in the asymptotic region of $qR_g > 2$. The first cumulant Γ describes the initial decay of the TCF, $g_1(q,t)$. A double logarithmic plot of $\Gamma/q^2 \equiv D_{app}(q)$ against qR_g gave a curve that lies between those for hard spheres and flexible coils. In contrast to linear chains, it showed an asymptotic slope of 0.80−0.85 instead of the theoretically expected slope of 1.00. The reduced first cumulant $\Gamma^*(q) \equiv (\Gamma/q^3)(\eta_0/kT)$ did not approach a constant plateau at large q but decayed continuously below the experimentally observed plateau value for linear chains. The reason for this behavior is seen in the high branching density and a loss of internal flexibility. In a second part, the angular dependence of the first cumulant in the semidilute regime, up to $c/c^* = 5$, was measured. The data from the different concentrations could be condensed to one common master curve when an empirical scaling parameter $\overline{R_h(c)}$ was used. A plot of the TCF's from the various concentrations as a function of $\Gamma(q,c,)t$ resulted in q-independent *shape functions* $g_1(\Gamma t)$, which gradually changed from Zimm to Rouse behavior when the concentration was increased beyond the overlap concentration c^*. This change is interpreted as a result of hydrodynamic screening.

Introduction

Dynamic light scattering (LS) is mostly used for a quick determination of translational diffusion coefficients. The procedure is simple for spherical particles or if the particles are small compared to the wavelength of the light used. Measurements at only one scattering angle are sufficient in these cases. A wrong answer is obtained, however, with large linear or branched *chain molecules* if measurements are made only at one angle, e.g., 90°. The translational diffusion coefficient is a macroscopic transport coefficient, but dynamic light scattering is actually a technique that registers all types of motions due to the thermal fluctuation of a system in thermodynamic equilibrium. If the measurements are made in the limit of small $q = (4\pi/\lambda)\sin(\theta/2)$ values such that $qR_g \ll 1$, with R_g the radius of gyration at zero concentration, the whole particle or macromolecule is seen. Under these conditions the translational motion of the center of mass is probed. As was shown by Einstein,[1,2] the correct translational diffusion coefficient is also obtained from Brownian motion and the molecular friction coefficient $f = 6\pi\eta_0 R_h$ according to the relationship

$$D = \frac{kT}{f} = \frac{kT}{6\pi\eta_0 R_h} \tag{1}$$

in which R_h is a hydrodynamic equivalent sphere radius. This Stokes−Einstein equation is of eminent importance, as it allows the description of an empirical transport coefficient by a molecular parameter that describes the dimensions of the molecule.

Dynamic LS measurements made under conditions of $qR_g > 2$, on the other hand, probe distances in a particle that are much smaller than the particle diameter. For most colloidal particles there will be no difference in the result for the diffusion coefficient when the measurements are made at 90° or any other scattering angle. These particles are essentially rigid, and thus only the translational motion of the center of mass can be observed. Some macromolecules are composed of linear, branched, or cross-linked chains, and these chains mostly possess a remarkable segmental mobility. These internal modes of motion are superimposed upon the translational motion[3] of the center of mass. The correct translational diffusion coefficient is now obtained only after extrapolating the data of Γ/q^2 to zero scattering angle,[3,4] where Γ is the first cumulant of the field time correlation function (TCF), $g_1(q,t)$, obtained by dynamic LS. The data of Γ/q^2 are angular dependent when objects with internal flexibility are studied and increase with the scattering angle. In these cases it is useful to define an apparent diffusion coefficient

$$\Gamma/q^2 \equiv D_{app}(q) \tag{2}$$

The extrapolation to zero scattering angle is facilitated by a result of perturbation calculations for small qR_g, which yielded a linear increase of $D_{app}(q)$ in terms of $q^2R_g^2$ that is given by[5]

$$D_{app}(q) = D_z[1 + C_h(q^2R_g^2) - ...] \tag{3}$$

Here, D_z is the z-average of the translational diffusion coefficient and C_h is a structure sensitive coefficient[5,6] that will be discussed in greater detail below.

Relationships have been developed also for the asymptotic region of very large qR_g. They were first derived by de Gennes[7] and Dubois-Violette and de Gennes[8] and further improved by Akcasu, Han, and Benmouna.[9] The theories are, however, restricted to

[⊗] Abstract published in *Advance ACS Abstracts,* October 1, 1997.

S0024-9297(96)01776-7 CCC: $14.00

Table 1. Main Molecular Parameters of the Degraded Starches Used in This Contribution[a]

sample	$10^{-6}M_w$ (g/mol)	R_g (nm)	10^5A_2 [(mol mL)/g^2]	10^8D_z (cm^2/s)	R_h (nm)	ρ	$[\eta]$ (mL/g)
LD16	1.7	48	6.0	6.2	35	1.37	47.5
LD12	5.2	70	2.8	3.5	62	1.14	71.4
LD19	14.5	113	1.3	2.6	84	1.35	93.2
LD18	43	180	0.82	1.4	150	1.2	133.2
LD17	64	190	0.60	1.0	215	0.88	130.2

[a] The parameter ρ is defined as R_g/R_h for the same molar mass M_w. The other quantities have the usual meaning.

linear and flexible chains. Although the applicability of the derived results to nonlinear systems may be questioned, these relationships remain to be a useful guide also for such structures. This expectation is based on the following persuasive arguments: At large qR_g only short sections of the macromolecule are seen. These sections can be assumed to consist of linear segments as long as the branching density is low. However, in a recent paper[10] we presented results from a number of randomly branched systems that exhibited characteristic deviations from the linear systems. The mobility was clearly reduced by the attachment of the short chain sections to branching points.[10]

The present contribution deals with dynamic light scattering in a rather wide range of concentration of degraded starch samples in 0.5 M NaOH solutions. The samples were the same as measured by static light scattering. The molecular parameters and the properties of the angular dependence of the scattered light were given in papers 1−3.[11] The results will be repeated here, only if needed; the main data of the five samples used in this study are given in Table 1. We will focus mainly on the following two questions:

(1) Can *all* of the degraded starch samples be described at small qR_g by eq 3 with the same C_h parameter?

(2) Can the angular dependence of the dynamic LS data at different concentrations be represented in a scaled form similar to those obtained by static LS data?

The first question is related to the properties of individual macromolecules at zero concentration and the second one to the behavior in semidilute solution. The present investigation is complex in several aspects. Two may be mentioned.

First, the dynamics of individual molecules may be considered. Synthetic linear chains are often so small in size that a range $qR_g > 2$ cannot be realized by LS. Here only the translational diffusion contributes to the time correlation function (TCF). In only a few cases have very long chains been synsthesized and studied in a region of $qR_g \cong 3$ and larger.[1,9,13−19] In that region the TCF of dynamic LS has already become solely dependent on the internal motions.[1,10] The latter are segmental motions with respect to the center of mass. Large sized macromolecules, on the other hand, are easily obtained with branched materials. The region of internal motions is here readily entered. However, the interpretation of data is difficult since no strict theory exists at present on the dynamics of branched macromolecules.

Second, the regime of semidilute solutions may be regarded. This regime is well understood for linear chains due to the scaling concept by de Gennes[20] and the analytic theory by Edwards.[21] The coils of linear chains can fully interpenetrate each other, but this is possible only with the shells at the outside of the branched macromolecules. The multiple branching makes a deeper penetration impossible. This fact has some unexpected effects on the internal dynamics.

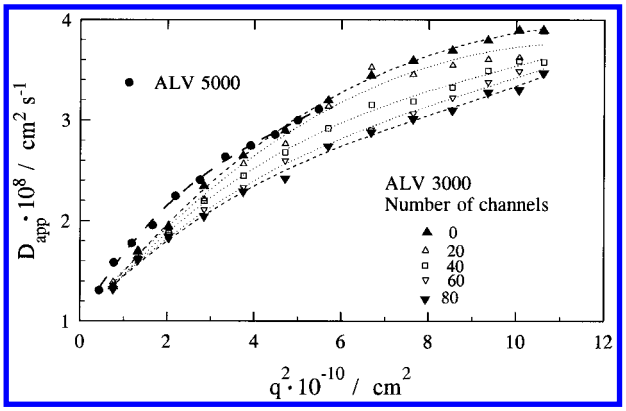

Figure 1. Effect of the channel number reduction on the apparent diffusion coefficient when using the ALV 3000 (linear) correlator and applying a three cumulant fit. Good agreement with the ALV 5000 correlator is obtained when extrapolating the ALV 3000 data to zero channel number (i.e., zero delay time).

Experimental Conditions

The dynamic light scattering measurements were carried out with an ALV instrument (ALV GmbH, Langen, Hessen, Germany) that was equipped with an ALV 3000 or ALV 5000 autocorrelator, respectively. All solutions were filtered three times through Millipore filters of 1.2, 0.8, 0.45, or 0.2 μm pore size, respectively, depending on the molar mass of the samples, the third time directly into the cylindrical light scattering cells of 0.8 cm in diameter. The cells were rinsed before use by freshly distilled acetone in a special rinsing apparatus to remove possibly adhered dust particles.

The dynamic measurements were first made with the ALV 3000 correlator that has a linear spacing of the delay times, and later with the ALV 5000 correlator in which the delay time is pseudologarithmically spaced; i.e., after each 8 linear time intervals the delay time is doubled; the total number of channels is 256. Within experimental errors the same translational diffusion coefficient was obtained with these two types of correlator, when the data were extrapolated to zero scattering angle.

At large scattering angles the apparent diffusion coefficients, defined by eq 2, displayed a strong angular dependence that was more pronounced for the high molar mass samples. Unfortunately, very different results were obtained with the ALV 3000 and ALV 5000 correlators, respectively, when a three-cumulant fit was applied to the data of the TCF at large scattering angles. The problem could be solved by reducing the number of channels. For the logarithmic ALV 5000 correlator we took care of the condition that (i) all cumulants had to be positive, and (ii) $\Gamma_2/2!$ should be almost equal in value with $\Gamma_3/3!$, where Γ_2 and Γ_3 are the second and third cumulants in the expansion of the field time correlation function $g_1(q,t)$ that is given by

$$\ln g_1(t,q) = \Gamma_0 - \Gamma_1 t + (\Gamma_2/2!)t^2 - (\Gamma_3/3!)t^3 + \ldots \quad (4)$$

$\Gamma_1 = \Gamma$ is the first cumulant that is connected with the apparent diffusion coefficient through the relationship of eq 3. The above quoted conditions were fulfilled for the ALV 5000 correlator when the time correlation function (TCF) has decayed not more than by 30% of its initial value. Consistent results were obtained with the ALV 3000 correlator when the number of channels was reduced to 20 channels. Figure 1 shows the effect of channel reduction for the measurements with the ALV 3000 correlator and the result from the ALV 5000 correlator.

Results and Discussion

Dilute Solutions: Behavior at Small qR_g. As was already mentioned in the introduction, the initial part

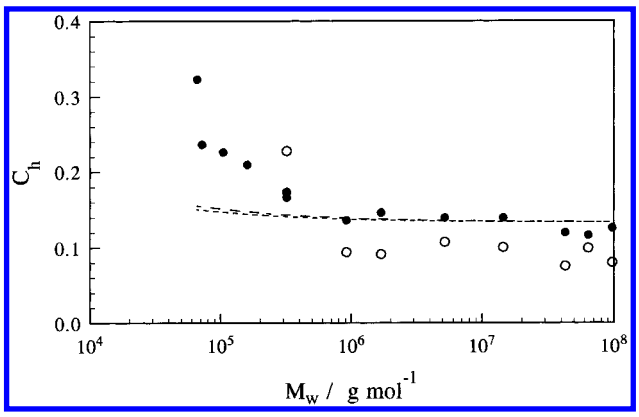

Figure 2. Molar mass dependence of the coefficient C_h in eq 2: (○) determined from R_g and the slope of $D_{app}(q)$; (●) according to eqs 5 and 6. The dashed lines correspond to the A-⟨^C_B polycondensation model with branching probabilities of $p = 0.016$ and $p = 0.024$.[11a,c]

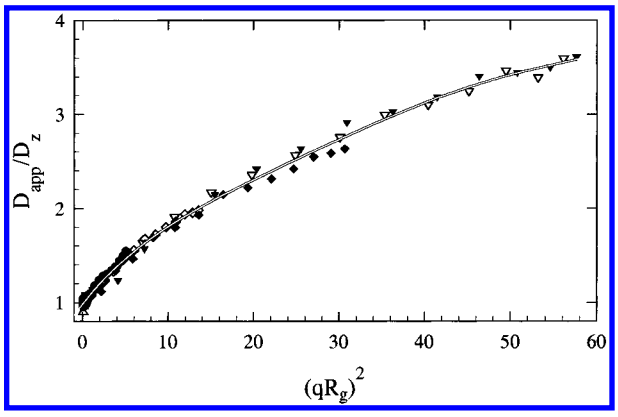

Figure 3. Plot of the normalized apparent diffusion coefficients $D_{app}(q)/D_z$ as a function of $(qR_g)^2$ for all samples with a detectable angular dependence. The C_h value is given here by the initial slope.

of the angular dependent apparent diffusion coefficient can be described by eq 3. In this equation the parameter C_h is related to the slowest mode of internal motion.[12] For flexible linear chains in a good solvent, which obey the Schulz−Flory size distribution, the value is $C_h = 0.2$.[5] Branching in general reduces this value,[5,6] e.g., to 0.102 for star molecules with many arms, but this decrease is partly compensated by a broad size distribution. For hard spheres the value is zero[1] and for thin stiff rods one has $C_h = 1/30 = 0.033$.[12] Evidently, a decrease in the C_h parameter indicates a decrease of the internal segment mobility. The internal modes of motions have to be distinguished from the local mobility. The local mobility is confined to the motions within segments that are not longer than one Kuhn segment. The internal motions, on the other hand, comprise much longer chain sections such that Gaussian statistics are still approximately fulfilled but the segments must be considerably shorter than the radius of gyration.[22,23]

The accurate determination of the C_h parameter is a difficult experimental task since this coefficient is the result from two initial slopes: The mean square radius of gyration is obtained from the initial slope in a Zimm plot of static LS data. The C_h coefficient, on the other hand, determines the slope of $D_{app}(q)$ against $(qR_g)^2$ (see eq 3).

Figure 2 shows the result of two procedures. In the first the initial slopes of the q^2 dependencies in static and in dynamic LS were determined, and C_h was calculated according to eq 2. In a second approach we applied a previously derived approximation[5,6,10]

$$D_{app}(q)/D_z \cong P_z(q)^{-\mu} \tag{5}$$

with

$$\mu = 3C_h \tag{6}$$

The validity of eq 6 is easily proven for $(qR_g)^2 \ll 1$ by using for the left hand side the approximation of eq 3 and for the right hand side the well-known series expansion of the particle scattering factor

$$P(q) \equiv \frac{R_\theta}{R_{\theta=0}} = 1 - \frac{1}{3}R_g{}^2q^2 + \ldots \tag{7}$$

Comparing the q^2 terms on both sides gives eq 6. R_θ and $R_{\theta=0}$ are the Rayleigh ratios of the scattered light at scattering angles θ and $\theta = 0$ (forward scattering), respectively. The extended validity of eq 6 for large qR_g is somewhat surprising but was found by numerical calculation of $D_{app}(q)$ and $P(q)$ by means of the cascade theory of branching.[5,6]

The two procedures gave for each of the five samples a surprisingly good agreement within deviations of $\Delta C_h = \pm 0.05$. Above $M_w = 5 \times 10^5$ g/mol, or $R_g = 30$ nm, a constant plateau value of $C_h = 0.11 \pm 0.02$ was obtained. This value agrees satisfactorily with the calculated one from the A-⟨^B_C polycondensation model (see appendix of part 3 of this series[11c]).

In a third approach we assumed that the scaled curve $D_{app}(q)/D_z$ is a universal function of $q^2R_g{}^2$ and holds for all starch fractions. Figure 3 shows the result for the five fractions that are large enough to develop an angular dependence. A common master curve is obtained for all samples. Estimations of the initial slope by different fitting procedures gave values between $C_h = 0.102$ and 0.134, which agree well with the average $C_h = 0.11 \pm 0.02$ obtained by the two other procedures.

These results allow us to answer the first question posed in the Introduction: The initial part of $D_{app}(q)/D_z$ is indeed universal for all degraded starch samples and can, within experimental errors, be described by a coefficient $C_h = 0.118 \pm 0.016$. The occurrence of a master curve as given by eq 5 is unexpected, since the particle scattering factors in static LS of these samples could *not* be transformed into one universal curve.

Dilute Solutions: Asymptotic Behavior. The observed angular dependence is a clear indication for internal segmental motions.[4,5,9,10] It is instructive to plot double logarithmically $D_{app}(q)/D_z$ against qR_g and to have a closer look at the asymptotic behavior.[4−10,13,14] Both variables in such a plot are dimensionless and are scaled quantities. Therefore, a certain universality can be expected. Figure 4 shows the result together with the curves for randomly branched or randomly cross-linked macromolecules. These curves are compared with those for linear chains in a good and poor solvent as predicted by theories.[15,19] As already mentioned, for large objects and at values of $qR_g > 3$ only internal motions should be detectable. For linear chains with strong hydrodynamic interactions one should find the response of the Zimm type of relaxation.[9,23] According to theories by de Gennes[7,8] and Akcasu[9] these Zimm modes give a q^3 dependence of the first cumulant Γ and a linear increase with q for $D_{app}(q)/D_z$ (Figure 4). Evidently, this is not the case for the branched samples. Systematic deviations occur in the asymptotic slope, and the curves are shifted to larger qR_g values. Instead of

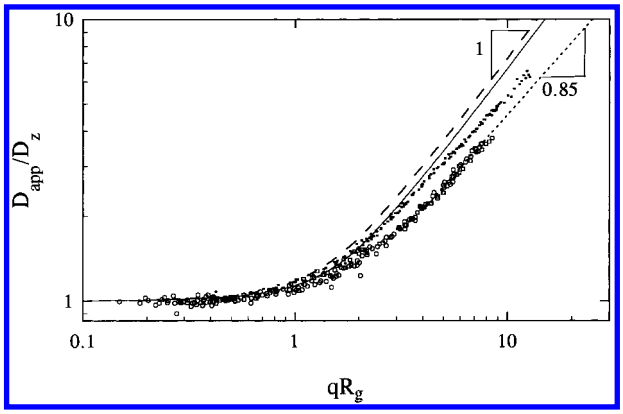

Figure 4. Double logarithmic plot of the normalized diffusion coefficients $D_{app}(q)/D_z$ against qR_g for the starch samples (lower curve) compared with those from randomly branched anhydride cured epoxies (polyesters) (middle curve) and the theoretically predicted ones for flexible linear chains in a good (- - -) and Θ solvent (—) respectively.

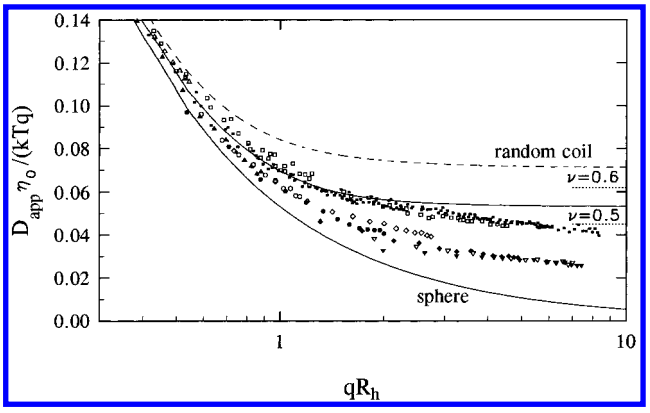

Figure 5. Plot of $\Gamma^*(q) = (\Gamma/q^3)(\eta_0/kT) = [D_{app}(q)]/q(\eta_0/kT)$ against qR_h for randomly branched samples (polyesters, polycyanates: data of the upper curve) and for the starch samples (lower curve). The results are compared with those predicted for random coils in good and Θ solvents indicated by $\upsilon = 0.6$ and 0.5, respectively. The dotted lines correspond to the experimentally observed limits.

a $q^{1.00}$ dependence, as expected for Gaussian segments, significantly lower exponents between 0.85 and 0.8 are found for the branched materials.[10] Furthermore, the shift to higher values of qR_g is considerably larger for the nonrandomly branched starch systems than for the randomly branched polymers that possess much lower branching densities. Interestingly, all data from the various starch fractions form one common curve if plotted against qR_g. A similar plot can be made using qR_h as abscissa; a larger shift and a lower exponent are obtained. (The split of the curves for $M_w < 40 \times 10^6$ g/mol results from the difficulties of determining the correct first cumulant with the ALV 3000 correlator.) The shift of the curves in Figure 4 to larger qR_g indicates that the internal motions in branched systems are detectable on a shorter length scale (larger q) than in coils of flexible linear chains. The effect becomes more pronounced as the branching density increases.

Further insight is obtained when the reduced first cumulant $\Gamma^*(q)$ is examined, which is defined as[14]

$$\Gamma^*(q) \equiv \left(\frac{\Gamma}{q^3}\right)\left(\frac{\eta_0}{kT}\right) = \left(\frac{D_{app(q)}}{q}\right)\left(\frac{\eta_0}{kT}\right) = \frac{1}{6\pi q\xi_h(q)} \quad (8)$$

(For linear chains $\Gamma^*(q)$ is just the prefactor of the q^3 dependence of Γ in the asymptotic limit.[9,15]) It may be noted that $\Gamma^*(q)$ is a dimensionless quantity. In contrast to $D_{app}(q)/D_z$, the scaling of the function $\Gamma^*(q)$ requires no polymer specific parameters for normalization. The hydrodynamic correlation length ξ_h is not further specified.[10,20] Figure 5 shows $\Gamma^*(q)$ as a function of qR_h. The theoretical curves for linear chains[15] in a good ($\nu = 0.6$) and a Θ-solvent ($\nu = 0.5$) are shown as dashed and full lines, respectively. The experimentally found asymptotes are indicated by the dotted lines. For comparison also the curve for hard spheres is shown. The experimental curves for the branched clusters fall between the two limits of flexible coils and hard spheres. This appears to be sensible since the branched clusters can be recognized as architectures between these two limits. The first cumulant Γ has the meaning of a reciprocal time. A decrease of $\Gamma^*(q)$, at a fixed q value, therefore means an increase in the relaxation time (slowing down of segmental motions) for chain sections of the same length. The slowing down observed with the branched macromolecules is equivalent to a loss in flexibility.

Another point of concern is the fact that all branched materials do not approach a constant plateau for large qR_h values, as should be the case when a Zimm type relaxation spectrum is present. Instead of approaching the expected q independence, a continuous decrease with a negative slope of approximately −0.2 is observed. Such a behavior may have the following two reasons.[10]

(i) One is that the covered qR_h region would be still too low for the asymptote. For systems of a high molecular polydispersity there is a considerable amount of low molar masses present for which even at high q-values the translational diffusion has a significant effect.[10] The translational diffusion contributes to the first cumulant with a power of q^2, and the corresponding $\Gamma^*(q)$ thus decreases $\sim q^{-1}$. Such an effect cannot be ruled out for randomly branched materials with their extremely large nonuniformity of size. For the starch samples, however, the size distribution is not exceedingly large.[11c,24]

The observed effect cannot be explained by a partial draining, because that would shift the relaxation times toward a Rouse type spectrum.[22] A Rouse spectrum results in a q^4 dependence[8,9] of the first cumulant or a linear *increase* with q for Γ*. Instead, a weak decrease is obtained.

(ii) The second explanation would indicate a change of the relaxation spectrum due to branching. At this point it may be recalled that all predictions made so far are deduced from theories on linear chains. The experimental findings with linear chains support this predicted behavior. It appears conceivable that branching introduces a much stronger perturbation to the simple spring−bead model of linear chains than has been anticipated. In fact, instead of being connected by only two springs to neighbors, the ends of a segment in a branched structure are actually connected by three or four springs. These attachments will result in strongly coupled motions for which the normal mode analysis is still fully unknown.[24] These additional springs inevitably must have an effect on the mobility.[25,26] Thus, we come to the conclusion that the Zimm relaxation spectrum is altered by branching or crosslinking. The effect is certainly small for long segments between two branching points but may become significant when the branching density is high.[10]

Semidilute Concentration Regime: Some General Remarks. In the past, much work has been done

on the chain dynamics of *individual linear* chains. A remarkable step forward in understanding was achieved by scaling concepts of de Gennes,[20] who applied these ideas to semidilute solutions. His predictions were quantified and cast into an analytic theory mainly by Edwards.[21] Both authors start with the assumption of fully interpenetrating coils. The experimental findings with linear chains strongly support this idea. For branched macromolecules a full interpenetrating of coils is not possible. The obstacles of branching points in shells at the outside of the macromolecules will allow only a partial interpenetration. Therefore, when the actual concentration is much higher than the overlap concentration, a much stronger influence of the interparticle interactions has to be expected. The effects of the thermodynamic interaction have been already reported and discussed in parts 2 and 3 of this series.[11a,b] In addition, hydrodynamic interactions have to be taken into account when the dynamics of the semidilute solution are examined.

Both types of interaction (thermodynamic and hydrodynamic) have an incisive influence on the measurable molecular parameters.[27,28] In a naive manner a molar mass or radius of gyration could be determined at a finite concentration in the same way as is known for infinite dilution. These so determined quantities are, however, only apparent ones and contain contributions arising from the osmotic force. In the following some of these apparent quantities are repeatedly used. Most of them were already defined and commented on in paper 3.[11c] For convenience, we simply list in the following the corresponding formulas without detailed comments.

Overlap Concentration c^*

$$c^* = 1/(A_2 M_w) \tag{9}$$

Apparent Molar Mass $M_{app}(c)$

$$\frac{1}{M_{app}(c)} = \frac{1}{RT}\left(\frac{\partial \pi}{\partial c}\right) = \frac{1}{M_w}[1 + 2A_2 M_w c + 3A_3 M_w c^2 + ...] \tag{10}$$

Apparent Radius of Gyration $R_{g,app}(c)$

$$R_{g,app}(c) \cong R_g(M_{app}(c)/M_w)^{1/2} = R_g[1 + 2A_2 M_w c + ...]^{-1/2} \quad \text{if} \quad c/c^* < 1 \tag{11a}$$

$$R_{g,app}(c) \cong R_g(A_2 M_w c)^{-1} \quad \text{if} \quad c/c^* > 1 \tag{11b}$$

Apparent Particle Scattering Factor $P_{app}(q,c)$

$$\frac{R_{q,c}}{R_{q=0,c}} \equiv P_{app}(q,c) = P_{app}[qR_{g,app}(c)] = P(qR_g) \tag{12}$$

where $R_{q,c}$ and $R_{q=0,c}$ are the Rayleigh ratios (scattering intensities) at concentration c and scattering vector values of q and $q = 0$, respectively. A_2 is the second osmotic virial coefficient, and the other quantities have the usual meaning.

Mutual (Collective) Diffusion Coefficient D_c and Hydrodynamic Correlation Length $\xi_h(c)$.

$$D_c = \frac{kT}{f(c)}\left[\frac{M_w}{M_{app}(c)}\right] \equiv \frac{kT}{6\pi\eta_0\xi_h(c)} \tag{13}$$

Apparent Mutual Diffusion Coefficient. Similar to infinite solution a first cumulant $\Gamma(q,c)$ can be measured at a given concentration c as a function of q (scattering angle). For flexible objects the ratio $\Gamma(q,c)/q^2$ will depend on q. Therefore, this ratio cannot be a true mutual diffusion coefficient D_c. Similar to eq 2 we define an apparent mutual diffusion coefficient

$$D_{app}(q,c) \equiv \Gamma(q,c)/q^2 \tag{14}$$

Equations 9−14 demonstrate the immense complexity of semidilute solutions: the naively defined apparent quantities depend on both the concentration c and the magnitude of the scattering vector q. The q dependence is equivalent to a ruler that tests the internal structure. Two further quantities come in when dealing with dynamics. These are the hydrodynamic interaction and the relaxation spectrum of segmental motions. Here the question arises whether this complexity can be simplified and contracted to rather universal master curves. The attempts in the following sections are directed to such a standardization. We consider the exploration of master curves as relevant, because deviations from a universal master curve, as the concentration is increased, will give clear indications for changes in the internal structure due to the thermodynamic and hydrodynamic interactions. These effects will allow distinguishing associated objects from molecularly dispersed ones.[28] The following treatment is confined to a selected sample of high molar mass.

Semidilute Solutions: Scaling of the Angular Dependent $D_{app}(q,c)/D_c$. In static LS the angular dependence of the apparent particle structure factor at different concentrations could excellently be transformed into one common master curve when $qR_{app}(c)$ was used as scaling parameter.[11c] The corresponding apparent diffusion coefficients exhibit very similar behavior to the static angular dependence. It was interesting to check whether similar scaling would be possible also for the dynamic LS measurements. Figure 6a shows the original experimental data of $D_{app}(c)$ against q^2 in a double logarithmic plot for the same sample (LD18: $M_w = 43 \times 10^6$ g/mol) and concentrations as used for static LS measurements in Figure 9 of paper 3. Strikingly, the six curves in Figure 6a show a common point of intersection (a range of concentrations from $0.5c^*$ to $5c^*$ was covered).

This intersection point is at variance to the findings with linear chains. For flexible linear chains all curves from different concentrations merge into one common line when the overlap concentration is exceeded. With increasing concentration the mesh size of the transitional network of interpenetrating chains becomes smaller. The asymptotic concentration independence observed with linear chains means that the local motions of the segments are not affected by the coil interpenetration.

In the present case, however, the motion at large q-values is slowed down when the concentration becomes larger than the overlap concentration due to growing restrictions. The common point of intersection indicates that the hindrance of segmental motion occurs at a well-defined length that can be estimated to lie between $1/qx = 70$ nm and $\xi_{hx} = 87$ nm where the latter is obtained from the apparent diffusion coefficient at that point, using the Stokes−Einstein relationship (the suffix x means crossing). The radius of gyration of this sample is $R_g = 180$ nm. From these values we may conclude that free interpenetration is possible only to a depth of 79 ± 8 nm. For shorter mesh sizes the freedom

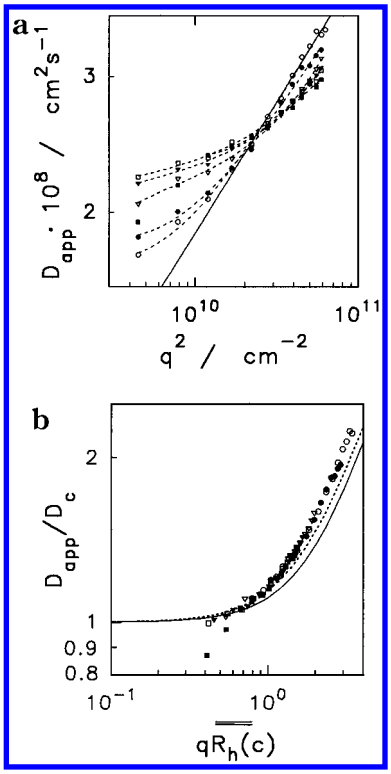

Figure 6. (a) Double logarithmic plot of the apparent mutual diffusion coefficient $D_{app}(q,c)$ against q^2 for six concentrations of sample LD18 ($M_w = 43 \times 10^6$ g/mol, $c^* = 2.8$ g/L), $c_1 = 1.3$ g/L, $c_6 = 12.7$ g/L. (b) Same data transformed into one common curve after normalization of $D_{app}(q,c)$ and shifting the curves to the position c_1. The shift factor is denoted as $\overline{R_h(c)}$. The lines correspond to the curve at $c = 0$ when scaled with R_g (dashed line) or R_h (full line), respectively.

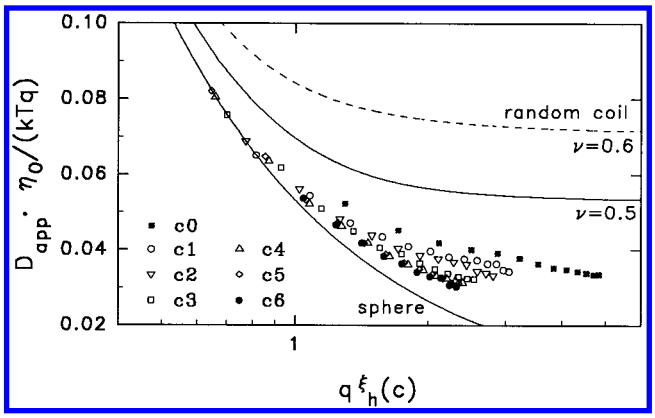

Figure 7. Plot of $\Gamma^*(q,c)$ against $q\xi_h$ for the six concentrations of Figure 6a.

of segmental motion becomes restricted. Apparently, this is a consequence of hindered interpenetration due to branching.

This conclusion is supported by Figure 7, which shows the reduced cumulant $\Gamma^*(c,q) \equiv (\Gamma/q^3)(\eta_0/kT)$ plotted against $q\xi_h(c)$ (eq 13). The curves are progressively pushed down to lower values as the concentration is increased. This again indicates a loss of mobility as has been shown recently in a detailed analysis of data from randomly branched[10] and aggregated chains.[28]

Attempts of constructing a master curve by using either $R_{g,app}(c)$ or ξ_h(c) as scaling parameters failed. A master curve could be found, however, by normalizing $D_{app}(q,c)$ with D_c and shifting the curves in Figure 6a of the high concentrations to that of the lowest concentration. (D_c is the mutual translational diffusion coefficient at concentration c that is obtained by extrapolation of $D_{app}(q,c)$ to zero scattering angle). The scaling parameter is denoted here as $\overline{R_h(c)}$. Figure 6b shows the final result that is compared with the result at zero concentration when qR_g (full line) and when qR_h (dashed line) is used (R_h is defined by eq 1).

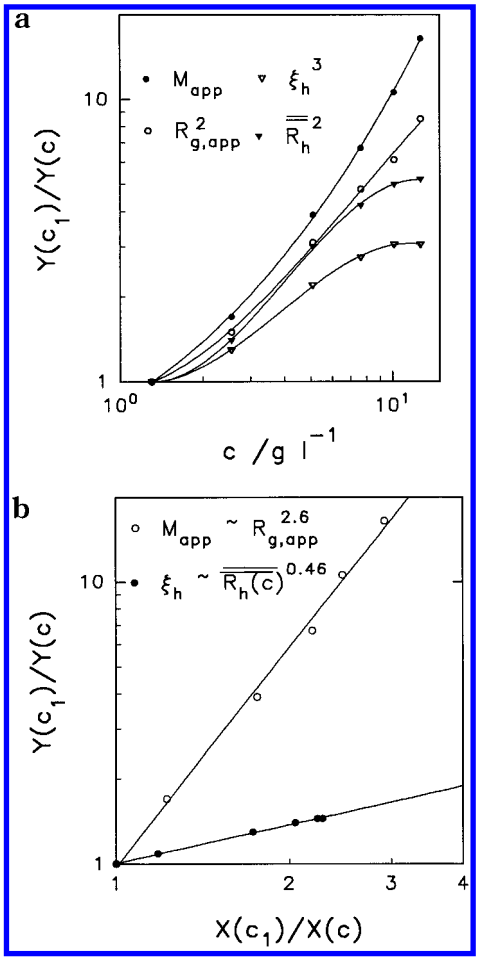

Figure 8. (a) Plot of $Y(c_1)/Y(c)$ against c, where $Y(c) =$ (●) $M_{app}(c)$, (○) $R_{g,app}{}^2$ (c), (▽) $\xi_h(c)$, (▼) $\overline{R_h}^2(c)$, respectively. (b) Double logarithmic plot of M_{app} against $R_{g,app}$ and ξ_h against $\overline{R_h(c)}$.

The scaling radius $\overline{R_h(c)}$ has a much stronger concentration dependence than the hydrodynamic correlation length $\xi_h(c)$ defined by eq 13 via D_c. Figure 8a shows the result in which also the concentration dependence of $M_{app}(c)$ is given. None of the three parameters displays power law behavior with regard to c.

However, good power law behavior is obtained when plotting $M_{app}(c)$ against $R_{g,app}(c)$ and $\xi_h(c)$ against $\overline{R_h(c)}$. The curves are shown in Figure 8b and follow the relationships

$$M_{app}(c) \propto [R_{g,app}(c)]^{2.6} \tag{15}$$

$$\xi_h(c) \propto [\overline{R_h(c)}]^{0.46} \tag{16}$$

The two equations (15) and (16) represent experimental findings with one selected sample of high molar mass $M_w = 43 \times 10^6$ g/mol. Another point is how these relationships are to be interpreted. Here we are entirely reliant on speculations since no theory on semidilute solutions of branched macromolecules has been proposed so far. The exponent in eq 15 could be interpreted as a fractal dimension, which is approximately the same as $d_f = 2.57$ that was obtained for the molar mass

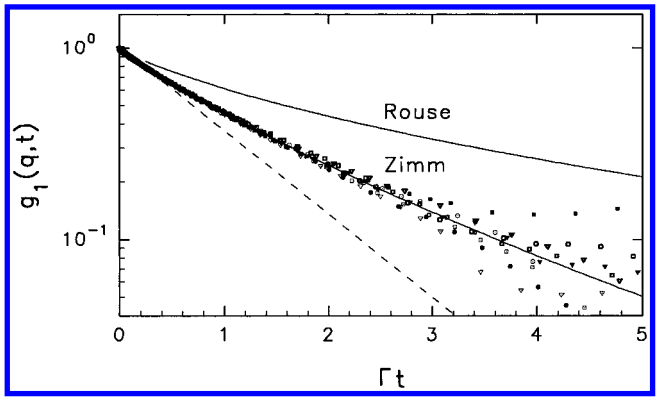

Figure 9. Plot of the logarithmic TCF, $g_1(q,t)$, against the scaled time $t/t^* = \Gamma(q)t$ for all samples and scattering angles obeying the condition $qR_g > 3$ at $c \rightarrow 0$.

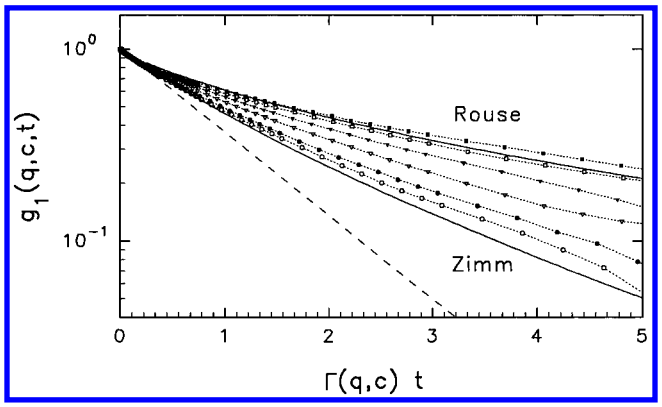

Figure 10. Concentration dependence of the shape functions from LD18 ($M_w = 43 \times 10^6$ g/mol. Lowest curve $c_1 = 1.3$ g/L, highest curve $c_6 = 12.7$ g/L; $c^* = 2.8$ g/L, $qR_g > 2$.

dependence of the radius of gyration.[11a] The remarkably low exponent in eq 16 is difficult to interpret since, so far, we have no clear idea on the physical meaning of the radius $\overline{R_h(c)}$. One possible explanation would be an effect of hydrodynamic screening, a conjecture that appears to be supported by findings of the next section.

Shape Function (Scaling of $g_1(q,c,t)$): Infinite Dilution. Since the early work by de Gennes[7] and Dubois-Violette[8] we know the approximate relationship for the field TCF, $g_1(q,t)$, at large qR_g for individual chains at $c = 0$. In a later study Akcasu and his colleagues[9] found that also the asymptotic TCF can be written in a scaled form using $t^* = 1/\Gamma(q)$ as scaling parameter, where $\Gamma(q)$ is the first cumulant of the TCF. A plot of $g_1(q,t)$ against the logarithm of t/t^* should therefore result in a function that is independent of q. The whole angular dependence is already included in the first cumulant. Because of this property Akcasu et al. called this function a *shape* function.[7,9] In their original paper they gave a list of numerically calculated shape functions for chains without (Rouse case) and with hydrodynamic interactions (Zimm case). Recent experiments showed that also branched macromolecules obeyed the relaxation spectrum of the Zimm type with strong hydrodynamic interaction.[10] Figure 9 demonstrates that also for the branched amylopectin in starch the condition of a shape function is fulfilled, if $qR_g > 2$. The experimental data are close to the curve for Zimm relaxation modes. This statement holds valid for individual macromolecules at infinite dilution.

Shape Function: Finite Concentrations. We now turn to finite concentrations in a range up to about 5c^*. A plot of the time correlation function $g_1(q,t,c)$ against $\Gamma(q,c)t$ gave for each concentration a q-independent curve, but now these curves gradually approached the Rouse limit for chains without hydrodynamic interaction when the concentration was increased. This is an indication for hydrodynamic screening.

Although a particle with $qR_g = 3$ was chosen, the condition $qR_{app} > 2$ is not fulfilled for the two highest concentrations because, according to eq 11, the apparent radius of gyration, R_{app}, decreases with c. An influence of the mutual translational diffusion coefficient, due to the polydispersity, cannot entirely be ruled out for these two concentrations. For very broad size distributions the shape of time correlation function at zero scattering angle is fully determined by the polydispersity and gives a function that deviates from the Zimm curve in the direction of the Rouse curve.[10] However, the size distribution of the sample is not exceptionally high,[29] in particular the ratio M_z/M_w never exceeds a value of 3 (appendix of paper 3[11c]) such that the influence of polydispersity can be disregarded, at least for the lower four concentrations in Figure 9.

Hydrodynamic screening was first observed in dynamic, spin-echo neutron scattering experiments by Stühn et al.[30] from polystyrene solutions in a concentration range of 10−60%. The findings with our sample seem to be the first example where hydrodynamic screening could be detected by dynamic LS. The reason why this behavior could be observed with the much lower concentrations of less than 10% probably results from the high segment density in this nonrandomly hyperbranched material. Further experiments have to be done to confirm this conclusion.

Conclusions

An angular dependence of the apparent diffusion coefficient $D_{app}(q) \equiv \Gamma/q^2$ is always observed when the particles possess some internal flexibility. Light scattering at large qR_g probes short distances in the macromolecule. Dynamic LS tests solely internal motions if $qR_g > 2$. It has been argued that in this limit *all* macromolecules will exhibit the same behavior. This argument is based on the fact that all macromolecules are built up of linear chain sections. At short distances (large q) mainly linear chain sections are seen. The present investigation now revealed that branching has an additional effect on the function $\Gamma^* = (\Gamma/q^3)(\eta_0/kT)$ and on the angular dependence of Γ and $D_{app}(q)$. The first cumulant of the branched system increases only with a power of $q^{2.8}$ instead of q^3 that was predicted and found for linear flexible chains. Probably the branching units influence the relaxation processes. The motions of the branching points are coupled with the spring-bead relaxations of a linear chain and could have a noticeable effect on the dynamics of the short chains connecting two branching units and could alter the common Zimm-Rouse spectra.[24] The effect will be noticeable only if the branching density is high, i.e., the interconnecting chains between two branching points are short.

Dynamic scaling of the angular dependence became possible for both samples of different M_w at infinite dilution and for solutions of starches at finite concentration up to about 5 times the overlap concentration c^*. The common static and dynamic correlation lengths are not suitable scaling parameters, but scaling could be achieved with a radius $\overline{R_h(c)}$. The successful scaling answers the two questions posed in the introduction: The measurements at different q and c, made with different starch samples, can indeed be universally

described. The strongly different concentration dependence of $\overline{R_h(c)}$ compared to that of $R_{g,app}(c)$ and of $\xi_h(c)$ remains, however, not sufficiently well understood.

The strongly q-dependent first cumulant of the field TCF $g_1(q,c,t)$ can, for each concentration, be transformed into a common shape function by choosing $\Gamma(q,c)t$ as a scaled delay time, t/t^*, if $qR_g > 2$. These shape functions change gradually their behavior from the Zimm to the Rouse type spectra, when the concentration is increased beyond the overlap concentration. The effect is interpreted as a result of hydrodynamic screening due to a high branching density.

Acknowledgment. We wish to thank Dr. Véronique Trappe for critical remarks and stimulating comments. This work was kindly supported by the Deutsche Forschungsgemeinschaft.

References and Notes

(1) Berne, B. J.; Pecora, R. *Dynamic Light Scattering*; Wiley: New York, 1976.
(2) Einstein, A. *Ann. Phys.* **1905**, *17*, 549.
(3) Pecora, R. *J. Chem. Phys.* **1964**, *40*, 1604; **1965**, *43*, 1562.
(4) Akcasu, Z. A.; Gurol, H. *J. Polym. Sci., Phys. Ed.* **1976**, *14*, 1.
(5) Burchard, W.; Schmidt, M.; Stockmayer, W. H. *Macromolecules* **1980**, *13*, 1265.
(6) Burchard, W. *Adv. Polym. Sci.* **1983**, *48*, 1 and references therein.
(7) De Gennes, P.-G. *Physics* **1967**, *3*, 37.
(8) Dubois-Violette, E.; de Gennes P.-G. *Physics* **1967**, *3*, 181.
(9) Akcasu, Z. A.; Benmouna, M.; Han, C. C. *Polymer* **1980**, *21*, 866.
(10) Trappe, V.; Bauer, J.; Weissmüller, M.; Burchard, W. *Macromolecules*, **1997**, *30*, 2365.
(11) Galinsky, G.; Burchard, W. *Macromolecules* **1995**, *28*, 2363 (part 1); **1996**, *29*, 1498 (part 2); **1997**, *30*, 4445 (part 3).
(12) Schmidt, M.; Stockmayer, W. H. *Macromolecules* **1984**, *17*, 509.
(13) Shiwa, Y.; Tsumashina, Y. *Physica A* **1994**, *197*, 47.
(14) Wiltzius, P.; Cannell, D. S. *Phys. Rev. Lett.* **1986**, *56*, 61.
(15) Benmouna, M.; Akcasu, Z. A. *Macromolecules* **1978**, *11*, 1187.
(16) Tsunashima, Y.; Hirata, M.; Nemoto, N.; Kurata, M. *Macromolecules* **1987**, *20*, 1992, 2862.
(17) Tsunashima, Y.; Nemoto, N.; Kurata, M. *Macromolecules* **1983**, *16*, 1184.
(18) Bhatt, M.; Jamieson, A. M.; Petschek, R. G. *Macromolecules* **1989**, *22*, 1374.
(19) Han, C. C.; Akcasu, Z. A. *Macromolecules* **1981**, *14*, 1080.
(20) De Gennes, P.-G. *Scaling Concepts in Polymer Physics*; Cornell University Press: Ithaca, NY, 1979.
(21) Doi, M.; Edwards, S. F. *The Theory of Polymer Dynamics*; Clarendon Press: Oxford, U.K., 1986.
(22) Rouse, P. E. *J. Chem. Phys.* **1953**, *21*, 1267.
(23) Zimm, B. H. *J. Chem. Phys.* **1956**, *24*, 269.
(24) Zimm, B. H.; Kilb, R. W. *J. Polym. Sci.* **1959**, *37*, 19.
(25) Harris, R. A.; Hearst, J. E. *J. Chem. Phys.* **1966**, *44*, 2595.
(26) Simon, E. J. *Chem. Phys.* **1970**, *52*, 3879.
(27) Burchard, W.; Lang, P.; Schulz, L.; Coviello, T. *Makromol. Chem., Macromol. Symp.* **1992**, *58*, 21.
(28) Burchard, W. *Adv. Colloid Interface Sci.* **1996**, *64*, 45.
(29) Erlander, S.; French, D. *J. Polym. Sci.* **1956**, *20*, 7.
(30) (a) Ewen, B.; Stühn, B.; Binder, K.; Richter, D.; Hayter, J. B. *Polym. Cummun.* **1984**, *25*, 133. (b) Richter, D.; Binder, K.; Ewen, B. ; Stühn, B. J. *Phys. Chem.* **1984**, *88*, 6618.

MA961776G